Differential Diversity-Embedding Space-Time Block Coding for 2 and 4 Transmit Antennas

Payam Rabiei, *Student Member, IEEE* and Naofal Al-Dhahir, *Fellow, IEEE*

***Abstract*—Diversity-Embedding Space-Time Block Coding (DE-STBC), introduced in [1], enables Unequal Error Protection (UEP) using multiple transmit antennas. Even though these codes do not require channel state information (CSI) at the transmitter, they do need it at the receiver for decoding. A novel differential DE-STBC scheme is proposed in this paper to eliminate the need for channel estimation at the receiver which is especially costly with multiple transmit and receive antennas. Most previously proposed differential schemes in the literature are based on orthogonal STBC and hence are not applicable to the non-orthogonal family of DE-STBC considered in this paper.**

***Index Terms*—Diversity embedding, differential detection decoding, throughput, unequal error protection, space-time coding.**

I. Introduction

ACCURATE channel state information (CSI) is required in a coherent communication system to enable reliable decoding at the receiver. Channel estimation, however, could be a difficult task especially in a multi-input multi-output (MIMO) systems. This is due to the increased number of channel parameters to be estimated while the total transmitted power stays the same. Eliminating channel estimation overhead and complexity motivates differential schemes [6], [7], [8], [11] at the expense of some performance loss. Most previous works on differential STBC, are based on Orthogonal STBC (OSTBC) [6], which utilize orthogonal matrices to encode information symbols and suffer the minimum performance loss (about 3-dB at high SNR) from coherent decoding. These works are not applicable to the non-orthogonal DE-STBC class of codes which provide an unequal error protection (UEP) capability by assigning different diversity levels to the information symbols [1], [3], [4]. By sacrificing some diversity for the less-important information symbols, an overall rate-increase is achieved. In DE-STBC, information symbols are transmitted in layers, each operating at a suitable rate-diversity trade-off point according to its quality of service (QoS) requirements. This establishes a form of wireless communications where the high-rate layer makes opportunistic use of good channel conditions to achieve high throughput, while the embedded high-diversity layer ensures that at least the high-priority symbols are decoded reliably. We emphasize that DE-STBC is an open-loop transmission scheme and hence CSI knowledge at the transmitter is not required. The objective of this paper is to design a differential DE-STBC scheme that eliminates the need for CSI at the receiver as well.

Manuscript received February 4, 2007; revised July 28, 2007; accepted October 28, 2007. The associate editor coordinating the review of this letter and approving it for publication was M. Win. This work was supported in part by the Texas Advanced Technology Program (ATP) under Contract 009741-0023-2003, and by the National Science Foundation (NSF) under Contracts CCF 04-30654 and DMS 05-28010, and by a gift from Texas Instruments Inc.

The authors are with the University of Texas at Dallas, Richardson, TX, USA (e-mail: {pxr054100, aldhahir}@utdallas.edu.

Digital Object Identifier 10.1109/TWC.2008.070139.

There are two major challenges in designing differential schemes for non-orthogonal STBC (such as DE-STBC). First, we need to properly normalize the transmitted codewords to ensure a fixed transmission energy and to guarantee that the generated codewords do not blow up or diminish with repeated application of the differential encoding rule. Furthermore, this energy-normalizing factor is time-varying and must be estimated and tracked at the receiver for reliable differential decoding. Second, due to the non-orthogonal nature of DE-STBC, the performance loss of the differential scheme from its coherent counterpart could be significant (more than the minimum 3 dB achieved with orthogonal STBC). In this paper, we study these two problems and propose effective solutions for both. The rest of the paper is organized as follows: in Section II we define the system model and introduce a DE-STBC design for 2 transmit antennas. In Section III, we present the mathematical formulation of the proposed differential scheme. Section IV generalizes our results to 4 transmit antennas and shows how to reduce the complexity of the naive exhaustive search decoding. In Section V, we discuss system design trade-offs. Finally, simulation results are provided in Section VI.

II. System Model

Consider a wireless communication system with $\boldsymbol{M}$ transmit antennas and $\boldsymbol{N}$ receive antennas over a Rayleigh flat-fading channel. The assumption of fixed channel during at least two block transmissions is necessary to establish reliable differential decoding at the receiver. The received signal is an $\boldsymbol{N} \times \boldsymbol{T}$ matrix R^k whose (n,t) element $r^k_{n,t}$ is the received symbol by antenna n at time slot t during kth block where $\boldsymbol{T}$ is the block time duration. We define U^k as the kth transmitted block of size $\boldsymbol{M} \times \boldsymbol{T}$ whose (m,t) element $u^k_{m,t}$ is the transmitted symbol by antenna m in time slot t. The channel is a quasi-static $\boldsymbol{N}\times \boldsymbol{M}$ matrix H^k whose entries are assumed to be the samples of independent complex Gaussian random variables with zero mean and variance of 0.5 per real dimension. We have

$$R^k = H^k U^k + Z^k \qquad (1)$$

where the elements of the noise vector Z^k are assumed to be zero-mean complex Gaussian random variables with variance $\sigma^2 = \frac{1}{2SNR}$ per real dimension. As a concrete example, we start with the following DE-STBC codeword design for 2 transmit antennas proposed in [3] and develop its differential encoding/decoding scheme and assume, for simplicity, one receive antenna ($\boldsymbol{N} = 1$).

$$C^k = \begin{bmatrix} a_0^k & b_0^k/\Gamma \\ -b_1^{k*}/\Gamma & a_0^{k*} \end{bmatrix} \tag{2}$$

where $(.)^*$ denotes complex conjugation, $a_0^k \in \mathcal{A}$ and $(b_0^k, b_1^k) \in \mathcal{B}$ are the kth information symbols carved from unit-energy QPSK signal sets $\mathcal{A}$ and $\mathcal{B}$, and $\Gamma > 1$ is an energy scaling factor to be optimized as a function of the constellation size.[1] It was shown in [3] that the diversity order of information symbol a_0^k is 2 while that of b_0^k and b_1^k is 1[2]. The bit error rate (BER) performance of both diversity layers depends on the choice of the scaling factor Γ. We will show that by proper choice of Γ, we can reduce the performance gap between coherent and differential decoding while ensuring that the performance of the lower-diversity layer $\mathcal{B}$ still satisfies a prescribed QoS level. The average transmitted energy in the proposed differential scheme is normalized during each block transmission where the energy normalizers are time-varying due to the non-orthogonal structure of the codewords. Therefore, they must be estimated at the receiver, which results in further performance loss due to estimation errors and the possible propagation of these errors through a received frame of data.

III. Differential Encoding and Decoding

In this section, we present our proposed differential encoding/decoding scheme.

A. Differential Encoding

As we discussed in the previous section, the total transmitted energy from all antennas is constrained to be a constant independent of $\boldsymbol{M}$; i.e.

$$\mathbf{E}\left[\sum_{t=1}^{T}\sum_{m=1}^{M}|u_{m,t}^k|^2\right] = T \tag{3}$$

where $\mathbf{E}[.]$ is the expectation operation. The differential scheme is initialized by transmitting $U^0 = I_2$, where I_2 is the 2×2 identity matrix, and proceeds as follows

$$V^k = U^{k-1}C^k \tag{4}$$

$$U^k = \frac{V^k}{\sqrt{e^k}} \tag{5}$$

where U^{k-1} and U^k are the transmitted codewords at times $k-1$ and k, respectively, and e^k is the energy normalizer i.e. $e^k = \frac{tr\{V^kV^{kH}\}}{T}$ where $tr\{.\}$ denotes the trace of the matrix and $(.)^H$ is the Hermitian transpose. Hence, the energy constraint in (3) is satisfied since

$$\begin{aligned}\mathbf{E}\left[\sum_{t=1}^{T}\sum_{m=1}^{M}|u_{m,t}^k|^2\right] &= \mathbf{E}\left[tr\left\{U^kU^{kH}\right\}\right] \\ &= \mathbf{E}\left[tr\left\{\frac{V^kV^{kH}}{\frac{tr\{V^kV^{kH}\}}{T}}\right\}\right] \\ &= \mathbf{E}\left[\frac{T}{tr\{V^kV^{kH}\}}tr\{V^kV^{kH}\}\right] \\ &= T\end{aligned} \tag{6}$$

The corresponding received signal vectors over block transmissions k and $k-1$ are

$$[R^k \quad R^{k-1}] = [H^kU^k \quad H^{k-1}U^{k-1}] + [Z^k \quad Z^{k-1}] \tag{7}$$

Substituting (4) and (5) into (7) and applying the quasi-static channel assumption i.e. $H^k = H^{k-1}$, the kth received signal block can be expressed in terms of the previously-received block as follows

$$R^k = \frac{R^{k-1}C^k}{\sqrt{e^k}} + \tilde{Z}^k \tag{8}$$

where

$$\tilde{Z}^k = Z^k - \frac{Z^{k-1}C^k}{\sqrt{e^k}} \tag{9}$$

which has a variance of

$$\tilde{\sigma}^2 = \sigma^2\left(1 + \frac{1}{Te^k}tr\{C^kC^{kH}\}\right) = \sigma^2\left(1 + \frac{(1+1/\Gamma^2)}{e^k}\right) \tag{10}$$

which shows that the equivalent noise variance seen by the differential decoder depends on Γ. Moreover, we can see from (2) and (10) that as Γ increases, C^k tends towards an orthogonal STBC with 3dB performance loss from coherent decoding. Note that $e^k = 1$ for orthogonal STBC and m-PSK constellations. Mathematically

$$\begin{aligned}\lim_{\Gamma\to\infty}\frac{tr\{C^kC^{kH}\}}{T} &= \lim_{\Gamma\to\infty}\frac{tr\left\{\begin{bmatrix} 1+\frac{1}{\Gamma^2} & \frac{a_0}{\Gamma}(b_0-b_1) \\ \frac{a_0^*}{\Gamma}(b_0^*-b_1^*) & 1+\frac{1}{\Gamma^2}\end{bmatrix}\right\}}{2} \\ &= \lim_{\Gamma\to\infty}\left(1+\frac{1}{\Gamma^2}\right) = 1\end{aligned} \tag{11}$$

B. Differential Decoding

Due to the non-orthogonality of DE-STBC, Maximum Likelihood (ML) decoding can not be performed using simple matched filtering as in orthogonal STBC and an exhaustive search is needed whose complexity increases exponentially with the constellation size and the number of transmit antennas. Starting from (7) we can derive the ML decoding rule for our non-orthogonal differential DE-STBC as follows

$$\begin{aligned}R &\triangleq \left[R^k \quad R^{k-1}\right] \\ &= H^k\left[U^k \quad U^{k-1}\right] + \left[Z^k \quad Z^{k-1}\right] \\ &= H^k\left[U^{k-1}D^k \quad U^{k-1}\right] + \left[Z^k \quad Z^{k-1}\right] \\ &= H^kU^{k-1}\left[D^k \quad I\right] + \left[Z^k \quad Z^{k-1}\right] \triangleq HG + Z\end{aligned} \tag{12}$$

where $H \triangleq H^kU^{k-1}$ and $D^k = \frac{C^k}{\sqrt{e^k}}$. Since $Z = \left[Z^k \quad Z^{k-1}\right]$ is AWGN and *independent* of G, we can write

[1]For simplicity, our focus in this paper is on QPSK signal constellations but our development is also applicable to any PSK constellation.

[2]These diversity orders assume coherent decoding. Deriving the diversity orders for differential decoding is more challenging since the non-orthogonal DE-STBC considered in this paper do not form a multiplicative group. Hence, repeated multiplication of the codewords during differential encoding causes the transmitted codewords to lose their special structure that enabled us to prove the diversity orders in the coherent case.

the exact ML decoding metric as follows

$$J_{ML} = \arg\min \|R - HG\|^2 \quad (13)$$

which can be equivalently written as

$$J_{ML} = \arg\min \left\{ \|R^k - HD^k\|^2 + \|R^{k-1} - H\|^2 \right\} \quad (14)$$

We can eliminate the dependence of J_{ML} on $H = H^k U^{k-1}$ by differentiating J_{ML} with respect to H to find the choice of H which minimizes J_{ML}. Using the following identity on the derivative of a quadratic function of a matrix with respect to that matrix

$$\frac{\partial (AX+b)^H C (DX+e)}{\partial X} = (DX+e)^H C^H A + (AX+b)^H CD$$

and equating to zero we get

$$\begin{aligned} 0 &= \frac{\partial J_{ML}}{\partial H^k U^{k-1}} \\ &= \frac{\partial \left(R^k - H^k U^{k-1} D^k\right)\left(R^k - H^k U^{k-1} D^k\right)^H}{\partial H^k U^{k-1}} \\ &+ \frac{\partial \left(R^{k-1} - H^k U^{k-1}\right)\left(R^{k-1} - H^k U^{k-1}\right)^H}{\partial H^k U^{k-1}} \\ &= \left(R^k - H^k U^{k-1} D^k\right)\left(-D^{kH}\right) + \left(R^{k-1} - H^k U^{k-1}\right)(-1) \\ &+ \left[\left(-D^k\right)\left(R^{kH} - D^{kH} U^{k-1H} H^{kH}\right)\right]^H \\ &+ \left[(-1)\left(R^{k-1H} - U^{k-1H} H^{kH}\right)\right]^H \\ &= 2\left(R^k - H^k U^{k-1} D^k\right)\left(-D^{kH}\right) - 2\left(R^{k-1} - H^k U^{k-1}\right) \\ &= -R^k D^{kH} + H^k U^{k-1} D^k D^{kH} - R^{k-1} + H^k U^{k-1} \\ &= -\left(R^k D^{kH} + R^{k-1}\right) + H^k U^{k-1}\left(I + D^k D^{kH}\right) \end{aligned} \quad (15)$$

Therefore, we can solve for the optimum choice of $H^k U^{k-1}$ from (15) to be

$$H^k U^{k-1} = \left(R^k D^{kH} + R^{k-1}\right)\left(I + D^k D^{kH}\right)^{-1} \quad (16)$$

Substituting back in (14) for $H^k U^{k-1}$, the exact ML differential decoding metric is given by

$$\begin{aligned} J_{ML} = \min &\left\| R^k - (R^k D^{kH} + R^{k-1})(I + D^k D^{kH})^{-1} D^k \right\|^2 \\ &+ \|R^{k-1} - (R^k D^{kH} + R^{k-1})(I + D^k D^{kH})^{-1}\|^2 \end{aligned} \quad (17)$$

This metric is very complex to implement so the *approximate* ML decoder can be derived by minimizing the suboptimal[3] metric from (8) as follows

$$J_{ML}^{\text{approx}} = \arg\min_{a_0^k, b_0^k, b_1^k} \left\| R^k - \frac{R^{k-1} C^k}{\sqrt{e^k}} \right\|^2 \quad (18)$$

The performance of J_{ML}^{approx} metric is compared with J_{ML} in Fig.5 for $\Gamma = 1.5$ and 3. It is seen that for $\Gamma = 1.5$, there is a small performance gap of about 0.5dB, however, as Γ increases, this gap becomes negligible. The reason is that J_{ML} collapses to J_{ML}^{approx} for orthogonal STBC[4] and m-PSK constellations and since for large Γ, the off-diagonal elements of C^k shrink to zero and the matrix becomes unitary, hence J_{ML}^{approx} and J_{ML} are equivalent. The estimate of e^k, at the receiver denoted by $\hat{e^k}$, is calculated by differentially re-encoding $\hat{C}^k$ when minimizing J_{ML}^{approx}

$$\overline{V^k} = \overline{U^{k-1}} \hat{C}^k \quad (19)$$

where $\overline{V^k}$ and $\overline{U^{k-1}}$ are the reconstructed matrices at the receiver, representing V^k and U^{k-1}, respectively. The estimate of e^k at the receiver is calculated as follows

$$\hat{e^k} = \frac{tr\{\overline{V^k V^{kH}}\}}{T} = \frac{\mathbf{E}\left[\sum_{t=1}^{T}\sum_{m=1}^{M} |\overline{v^k}_{m,t}|^2\right]}{T} \quad (20)$$

Error propagation could arise here because the *estimated* codeword $\hat{C}^k$ is used to calculate $\overline{V^k}$.

IV. Extension to 4-Transmit Antennas

In this section, we present a DE-STBC construction for 4 transmit antennas which allows a reduced-complexity hybrid maximum likelihood interference cancellation (HMLIC) decoding at the receiver without any performance loss from the approximate ML decoding rule in (18). The codeword for the 2-transmit-antenna case in (2) is used as a building block to form a 4×4 codeword as follows

$$C_{4\times4}^k = \begin{bmatrix} \mathbf{A}^k & C^k \\ (C^k)^H & (\mathbf{A}^k)^H \end{bmatrix} = \begin{bmatrix} a_0^k & a_1^k & a_2^k & b_0^k/\Gamma \\ -a_1^{k*} & a_0^{k*} & -b_1^{k*}/\Gamma & a_2^k \\ a_2^{k*} & -b_1^k/\Gamma & -a_0^{k*} & a_1^k \\ b_0^{k*}/\Gamma & -a_2^{k*} & a_1^{k*} & a_0^k \end{bmatrix} \quad (21)$$

where $\mathbf{A}^k$ is a 2×2 Alamouti codeword [2]. We define two diversity layers $\mathcal{A}$ and $\mathcal{B}$ where $(a_0^k, a_1^k, a_2^k) \in \mathcal{A}$ and $(b_0^k, b_1^k) \in \mathcal{B}$. The rates of layers $\mathcal{A}$ and $\mathcal{B}$ are $\frac{3}{4}$ and $\frac{1}{2}$, respectively, and the total code rate is $\frac{5}{4}$. It can be shown [4] that with ML coherent decoding, diversity orders of 4 and 2 are achieved by Layers $\mathcal{A}$ and $\mathcal{B}$, respectively. The HMLIC decoding algorithm performs an exhaustive search over layer $\mathcal{B}$ symbols followed by canceling their interference from the original received vector. Then, layer $\mathcal{A}$ symbols are decoded by performing a simple matched filtering (MF) operation. Since the equivalent channel matrix (after canceling the interference from layer $\mathcal{B}$) is *orthogonal*, no performance loss is incurred due to MF operation. Finally, from all the codeword candidates, we select the one that results in the smallest value for the approximate simple ML metric in (18). Assuming one receive antenna, the received signal is given by

$$R^k = \frac{R^{k-1} C_{4\times4}^k}{\sqrt{\hat{\varepsilon^k}}} + \hat{Z}^k \quad (22)$$

where $\hat{\varepsilon^k}$ is the energy normalizer estimate for the 4-transmit-antenna code. Note that $\hat{\varepsilon^k}$ can be computed analogous to $\hat{e^k}$ in (20). The modified received symbols are computed by cancelling the interference of the decoded symbols $(\hat{b}_0^k, \hat{b}_1^k)$ from the original received vector as follows

$$\begin{aligned} {r'}_1^k &= r_1^k - r_4^{k-1}\frac{\hat{b}_0^{k*}}{\Gamma\sqrt{\varepsilon^k}} \;;\; {r'}_2^k = r_2^k + r_3^{k-1}\frac{\hat{b}_1^k}{\Gamma\sqrt{\varepsilon^k}} \\ {r'}_3^k &= r_3^k + r_2^{k-1}\frac{\hat{b}_1^{k*}}{\Gamma\sqrt{\varepsilon^k}} \;;\; {r'}_4^k = r_4^k - r_1^{k-1}\frac{\hat{b}_0^k}{\Gamma\sqrt{\varepsilon^k}} \end{aligned} \quad (23)$$

[3]This metric is suboptimal since the equivalent noise term $\tilde{Z}^k$ in (8) is not white and is dependent on C^k as evident from (9).

[4]This can be easily verified by substituting $D^k D^{kH} = I_2$ in (17).

The matched-filtering operation is performed by re-arranging the resulting signal vector in the following form

$$\begin{aligned} R^{'k} &\triangleq \left(r_1^{'k}, r_2^{'k}, r_3^{'k}, r_4^{'k}, r_1^{'k*}, r_2^{'k*}, r_3^{'k*}, r_4^{'k*}\right)^T \\ &= \widetilde{R}^{k-1}\left(a_0^k, a_1^k, a_2^k, a_0^{k*}, a_1^{k*}, a_2^{k*}\right)^T + \overline{Z^k} \end{aligned} \quad (24)$$

where $\widetilde{R}^{k-1}$ can be viewed as the equivalent channel matrix and has the following orthogonal form

$$\begin{bmatrix} r_1^{k-1} & 0 & 0 & 0 & -r_2^{k-1} & r_3^{k-1} \\ 0 & r_1^{k-1} & 0 & r_2^{k-1} & 0 & -r_4^{k-1} \\ 0 & 0 & r_1^{k-1} & -r_3^{k-1} & r_4^{k-1} & 0 \\ r_4^{k-1} & r_3^{k-1} & r_2^{k-1} & 0 & 0 & 0 \\ 0 & -r_2^{k-1*} & r_3^{k-1*} & r_1^{k-1*} & 0 & 0 \\ r_2^{k-1*} & 0 & -r_4^{k-1*} & 0 & r_1^{k-1*} & 0 \\ -r_3^{k-1*} & r_4^{k-1*} & 0 & 0 & 0 & r_1^{k-1*} \\ 0 & 0 & 0 & r_4^{k-1*} & r_3^{k-1*} & r_2^{k-1*} \end{bmatrix}$$

Multiplying both sides of (24) by $(\widetilde{R}^{k-1})^H$ we get

$$(\widetilde{R}^{k-1})^H R^{'k} = \left(\sum_{i=1}^{4} |r_i^{k-1}|^2\right)\Omega + (\widetilde{R}^{k-1})^H Z^k \quad (25)$$

where $\Omega = \left(a_0^k, a_1^k, a_2^k, a_0^{k*}, a_1^{k*}, a_2^{k*}\right)^T$. The HMLIC decoding algorithm achieves the same performance as the approximate ML decoding while reducing the decoding complexity (for QPSK) from a size-4^5 exhaustive ML search to a size-16 ML search followed by a simple matched-filtering operation for each candidate codeword.

V. The Energy Scaling Factor Γ

Designing Γ in (2) and (21) involves a tradeoff between the following conflicting objectives

1) Minimizing the performance gap between differential and coherent decoding.
2) Minimizing the performance loss due to estimation of the energy normalizer e^k at the receiver.
3) Satisfying target BERs of diversity layers $\mathcal{A}$ and $\mathcal{B}$.
4) Maximizing the throughput and reducing the SNR crossover point with OSTBC (c.f. Fig. 3).

Eigenvalue analysis [5] provides an accurate performance measure for non-orthogonal STBC design (such as the DE-STBC considered in this paper). Assume $B(c, c^{'})$ is the difference between two non-orthogonal codewords c and $c^{'}$, then the closer the eigenvalues of $B(c, c^{'})B^H(c, c^{'})$ are to each other and to $tr\left[B(c, c^{'})B^H(c, c^{'})\right]/T$, the better the BER performance of both the differential and coherent schemes will be. The limiting case is the OSTBC where those eigenvalues become identical. Assuming a unit-energy QPSK constellation, we can calculate λ_1 and λ_2, the eigenvalues of $C^k C^{kH}$, as follows

$$\begin{aligned} 0 &= \det\left(C^k C^{kH} - \lambda \boldsymbol{I}_2\right) \\ &= \det\begin{pmatrix} 1 + \frac{1}{\Gamma^2} - \lambda & \frac{a_0}{\Gamma}(b_0 - b_1) \\ \frac{a_0^*}{\Gamma}(b_0^* - b_1^*) & 1 + \frac{1}{\Gamma^2} - \lambda \end{pmatrix} \\ &\Rightarrow \lambda_{1,2} = 1 + \frac{1}{\Gamma^2} \pm \frac{\sqrt{2}}{\Gamma}\sqrt{1 - \Re(b_0 b_1^*)} \end{aligned} \quad (26)$$

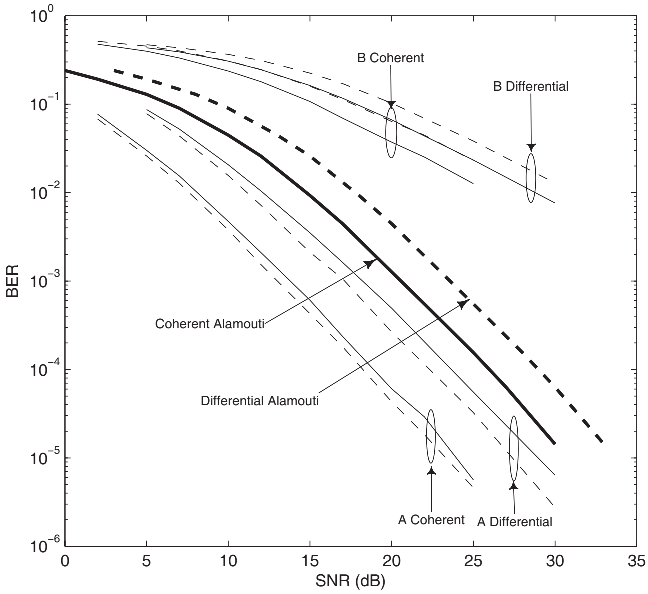

Fig. 1. BER performance for differential and coherent decoding of Layers $\mathcal{A}$ and $\mathcal{B}$ for 2 TX design.

The third term in (26) above is the absolute value of the off-diagonal elements of $C^k C^{kH}$. As Γ increases, both λ_1 and λ_2 tend to 1 which corresponds to a 3dB performance gap from coherent decoding.

For the DE-STBC design in (2) with QPSK modulation, as we increase Γ up to 3, the eigenvalues of $B(c, c^{'})B^H(c, c^{'})$ approximately approach the same value which satisfies our first design objective. However, further increase in Γ, reduce the receiver's capability to decode (b_0^k, b_1^k) and hence it fails to meet the target BER of diversity layer $\mathcal{B}$ which is the third design objective. Moreover, the SNR crossover point shown in Fig. 3 between the throughput curves of the proposed DE-STBC differential scheme and the Alamouti differential scheme, occurs at higher SNR values as we increase Γ. Our simulations show that the minimum SNR crossover point is achieved by choosing $\Gamma = 1.5$. Further decrease in Γ from 1.5 towards 1 results in unacceptable performance for layer $\mathcal{A}$ which also increases the SNR cross-over point in the throughput plot in Fig.3 from its minimum value achieved by $\Gamma = 1.5$. Based on the above observations, we conclude that a range of $1.5 < \Gamma < 3$ can be adopted and the exact value of Γ in this range depends on which of the four design objectives we want to emphasize more. More specifically, a higher throughput can be achieved by choosing Γ closer to 1.5 while a smaller BER gap is obtained by selecting Γ near 3. Table I quantifies these design tradeoffs when the target BERs of Layers $\mathcal{A}$ and $\mathcal{B}$ are set to 10^{-4} and 10^{-2}, respectively. It is worth emphasizing that the reported coherent decoding performance assumes perfect CSI at the receiver. With practical channel estimation effects, the performance gap between differential and coherent decoding will be further reduced.

VI. Simulation Results

In this section, we present our simulation results for the DE-STBC designs for $\boldsymbol{M} = 2$ and 4 transmit antennas given

TABLE I
REQUIRED SNR VALUES FOR DIFFERENTIAL AND COHERENT DECODING OF LAYERS $\mathcal{A}$ AND $\mathcal{B}$ FOR 2 TX DESIGN IN (2). TARGET BERS FOR LAYERS $\mathcal{A}$ AND $\mathcal{B}$ ARE 10^{-4} AND 10^{-2}, RESPECTIVELY

Scaling Factor Γ	1.5	2	3	4
Coherent A (dB)	23.2	21	18.9	18.22
Coherent B (dB)	22.3	23	26	28.9
Differential A (dB)	29.7	28	23.6	22.3
Differential B (dB)	26.3	26.7	28.9	31.5
SNR Gap A (dB)	6.5	7	4.7	4.08
SNR Gap B (dB)	4	3.7	2.9	2.6

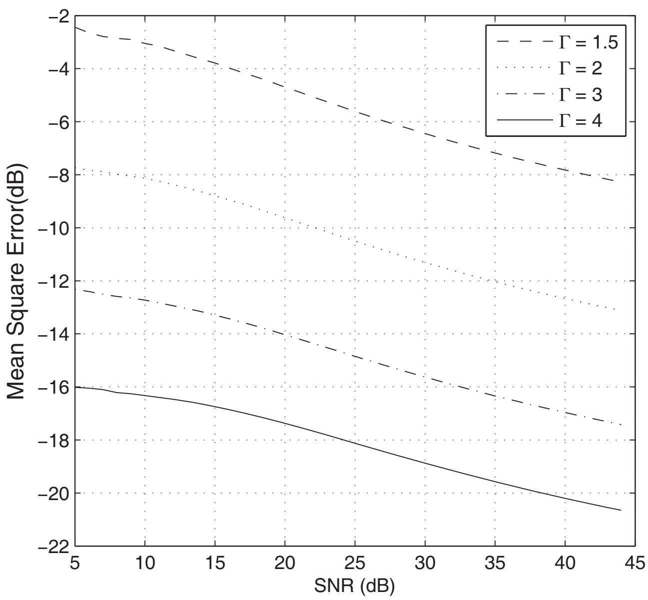

Fig. 2. Mean square error in estimating the energy normalizer e^k at the receiver for 2 TX design.

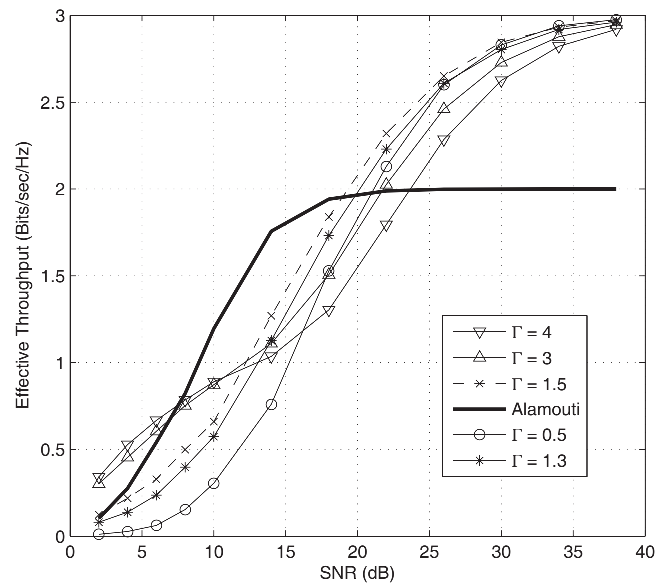

Fig. 3. Throughput comparison between differential decoding of the Alamouti STBC and our 2 TX DE-STBC for different values of Γ.

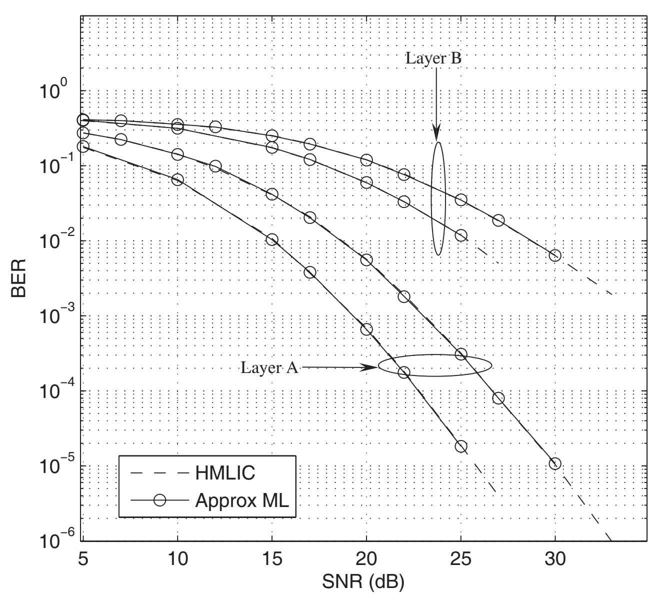

Fig. 4. BER performance comparison between HMLIC and approximate ML decoding for 4 TX design $C^k_{4\times 4}$ at $\Gamma = 1.5$.

earlier. We compare the BER performance of each design in differential and coherent transmission scenarios. First, to illustrate the effect of Γ on performance, we plot the BER of the 2-transmit-antenna design for $\Gamma = 3$ and 4. Fig. 1 compares the BER performance of diversity layers $\mathcal{A}$ and $\mathcal{B}$ with coherent and differential decoding where it is clear that the performance gap between the two schemes decreases as Γ increases (see Table I). The BER performance for differential and coherent Alamouti decoding is also given as a benchmark. The transmission rate of both codes is 3 bits/sec/Hz and the performance of the Alamouti scheme is sandwiched between that of layers $\mathcal{A}$ and $\mathcal{B}$ as expected. Fig. 2 shows that the mean square error (MSE) in estimating the energy normalizer e^k at the receiver (for the 2-transmit-antenna design) decreases as Γ and/or SNR increases. Fig. 3 compares the throughput of the DE-STBC design in (2) with that of the Alamouti STBC assuming differential transmission where it can be seen that the former outperforms the latter for medium to high SNR. The SNR cross-over point is around 19 dB for $\Gamma = 1.5$. Since this input SNR level is known at the transmitter, we can switch between the two codes to achieve the highest throughput for all SNR levels. Fig. 4 illustrates the BER performance of the 4×4 codeword $C^k_{4\times 4}$ in (21) for both diversity layers using HMLIC decoding. Approximate ML decoding using the metric in (18) is also compared with HMLIC decoding for $\Gamma = 1.5$ to confirm that no performance loss in incurred by using the reduced-complexity HMLIC decoder. Finally, Fig. 5 compares the performance of J_{ML} and J^{approx}_{ML} metrics for 2 TX design for $\Gamma = 1.5$ and 3 where we observe a small performance loss when $\Gamma = 1.5$. However, for $\Gamma = 3$, their performance becomes indistinguishable.

VII. CONCLUSIONS

We proposed a novel differential transmission scheme for diversity-embedding STBC for 2 and 4 transmit antennas where neither the transmitter nor the receiver have chan-

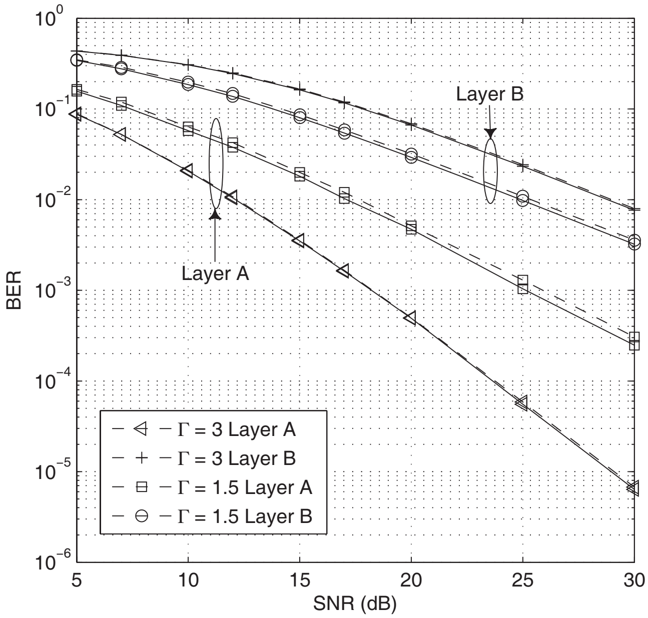

Fig. 5. Performance comparison between exact (J_{ML} solid lines) and approximate (J_{ML}^{approx} dashed lines) ML decoding for 2 TX design and $\Gamma = 1.5, 3$.

nel knowledge. Since the DE-STBC codewords are non-orthogonal, a time-varying energy-normalizing factor is introduced at the transmitter to ensure fixed-energy codewords. We optimize the DE-STBC code design to satisfy target BER performance levels for both diversity layers while maximizing the throughput and minimizing the performance gap between differential and coherent decoding. Extensions to frequency-selective channels can be pursued by carefully integrating the proposed scheme with orthogonal frequency division multiplexing (OFDM) [12], [13], [14], [15].

VIII. Acknowledgment

We are grateful for the Editor and the anonymous reviewers for their comments which improved the quality of the paper.

References

[1] S. N. Diggavi, N. Al-Dhahir, A. R. Calderbank "Diversity embedded space-time codes," in *Proc. Global Telecommunications Conference, 2003*, vol. 4, pp. 1909–1914.

[2] S. M. Alamouti, "A simple transmit diversity technique for wireless communications," *IEEE J. Select. Areas Commun.*, vol. 16, pp. 1451–1458, Oct. 1998.

[3] S. Das, N. Al-Dhahir, S. Diggavi, and A. R. Calderbank, "Opportunistic space-time block codes," in *Proc. IEEE Vehicular Technology Conference 2005*, vol. 3, pp. 2025–2029.

[4] S. Das and N. Al-Dhahir, "New diversity-embedding STBC constructions," in *Proc. IEEE Workshop on Signal Processing Advances in Wireless Communication SPAWC 2006*.

[5] O. Tirkkonen and A. Hottinen, "Improved MIMO performance with non-orthogonal space-time block codes," in *Proc. IEEE Global Telecommuncations Conference 2001*, vol. 2, pp. 1122–1126.

[6] V. Tarokh and H. Jafarkhani, "A differential detection scheme for transmit diversity," *IEEE J. Select. Areas Commun.*, vol. 18, no. 7, pp. 1169–1174, July 2000.

[7] B. M. Hochwald and W. Sweldens, "Differential unitary space-time modulation," *IEEE Trans. Communn.*, vol. 48, no. 12, pp. 2041–2052, Dec. 2000.

[8] B. L. Hughes, "Differential space-time modulation," *IEEE Trans. Inform. Theory*, vol. 46, no. 7, pp. 2567–2578, Nov. 2000.

[9] Y. Zhu and H. Jafarkhani, "Differential modulation based on quasi-orthogonal codes," *IEEE Trans. Wireless Commun.*, vol. 4, no. 6, pp. 3018–3030, Nov. 2005.

[10] G. Bauch and A. Mengi, "Non-unitary orthogonal differential space-time modulation with non-coherent soft-output detection," in *Proc. Vehicular Technology Conference*, vol. 2, pp. 977–981, Sept. 2005.

[11] C. Yuen, Y. L. Guan, and T. T. Tjhung, "Differential transmit diversity based on quasi-orthogonal space-time block code," in *Proc. IEEE Global Telecommunications Conference*, Nov. 2004.

[12] S. Diggavi, N. Al-Dhahir, A. Stamoulis, and A. R. Calderbank, "Differential space-time block-coding for frequency-selective channels," *IEEE Commun. Lett.*, vol. 6, no. 6, pp. 253–255, June 2002.

[13] H. Li, "Differential space-time modulation over frequency-selective channels," *IEEE Trans. Signal Processing*, vol. 53, no. 6, pp. 2228–2242, June 2005.

[14] D. Wang, H. Minn, and N. Al-Dhahir, "An opportunistic STBC-OFDM scheme with reduced PAR in the presence of frequency offset," in *Proc. IEEE Conference on Acoustics, Speech, and Signal Processing*, Apr. 2007.

[15] A. F. Molisch, M. Z. Win, and J. H. Winters, "Space-time-frequency coding for MIMO-OFDM systems," *IEEE Commun. Lett.*, vol. 6, no. 9, pp. 370–372, Sept. 2002.